Local Insulin-like Growth Factor I expression is essential for Purkinje neuron survival at birth

G. Giacomo Consalez, Laura Croci, Valeria Barili, Dennis Chia, Luca Massimino, Ruben van Vugt, Giacomo Masserdotti, Renato Longhi, Peter Rotwein

Local Insulin-like Growth Factor I expression is essential for Purkinje neuron survival at birth

Laura Croci[1#], Valeria Barili[2#], Dennis Chia[3], Luca Massimino[1,2], Ruben van Vugt[2], Giacomo Masserdotti[2], Renato Longhi [4] Peter Rotwein[3] and G. Giacomo Consalez[1§]

[1] San Raffaele Scientific Institute, Milan, Italy

[2] Vita-Salute San Raffaele University, Milan, Italy

[3] Oregon Health and Science University, Portland, OR, USA

[4] Consiglio Nazionale delle Ricerche, Milan, Italy

Joint first authors

Short title: local IGF1 fosters PC survival at birth.

§ to whom correspondence should be addressed at:
Division of Neuroscience
San Raffaele Scientific Institute
Via Olgettina 58
20132 Milano
Italy
Phone: +39 02 2643 4838
Fax: +39 02 2643 5283
email: g.consalez@hsr.it

ABSTRACT

Insulin-like growth factor I (IGF1), an anabolic and neuroprotective factor, promotes neuronal survival by blocking apoptosis. It is released into the bloodstream by the liver, or synthesized locally by muscles and neural cells, acting in an autocrine or paracrine fashion. Intriguingly, genetic studies conducted in invertebrate and murine models also suggest that an excess of IGF1 signaling may trigger neurodegeneration. This emphasizes the importance of gaining a better understanding of the mechanisms controlling IGF1 regulation and gene transcription. In the cerebellum, *Igf1* expression is activated just before birth in a subset of Purkinje cells (PCs). Mice carrying a null mutation for the helix-loop-helix (HLH) transcription factor Early B-cell factor 2 (EBF2) feature PC apoptosis at birth. We show that *Igf1* is sharply downregulated in *Ebf2* null PCs starting prior to the onset of PC death. *In vitro*, EBF2 binds a conserved distal *Igf1* promoter region. The pro-survival phosphoinositol-3-kinase (PI3K) signaling pathway is strongly inhibited in mutant cerebella. Finally, *Ebf2* null organotypic cultures respond to IGF1 treatment by inhibiting PC apoptosis. Consistently, wild type slices treated with an IGF1 competitor feature a sharp increase in PC death. Our findings reveal that IGF1 is required for PC survival in the neonatal cerebellum, and identify a new mechanism regulating its local production in the central nervous system.

INTRODUCTION

Apoptosis is a controlled by regulatory pathways that are strikingly conserved in metazoan evolution (e.g. see 1). The signaling pathways responsible for apoptosis are triggered both intracellularly, in response to a variety of stressful stimuli, and extracellularly, by proapoptotic ligands (e.g. see 2, 3) (reviewed in 4, 5).

Plentiful evidence shows that programmed cell death is required for the appropriate completion of neural development in many species, as exemplified by apoptosis of Rohon Beard primary sensory neurons in *Xenopus* embryos at metamorphosis (6, 7), and by the dramatic effects of CED-4/Apaf1 mutation in *C. elegans* (8) and mice (9). In the developing mouse cerebellum, a considerable percentage of PC progenitors born in the ventricular zone undergoes apoptosis; accordingly, in transgenics overexpressing the anti-apoptotic factor *Bcl2*, PCs are substantially increased in number (10).

While many neural cells are programmed to die in development, many others use antiapoptotic pathways for their survival during ontogenesis. Pro survival factors can act in a paracrine or autocrine fashion. Some are target-derived, and the competition for limiting amounts of neurotrophic signals produced by postsynaptic targets dictates the selection of their presynaptic afferents (11), while others act anterogradely (12). A large collection of secreted proteins has been found to promote neuronal survival in development. These molecules range from neurotrophins to various classes of trophic factors and cytokines (13).

Several authors have shown that, in many of the mouse mutants in which Purkinje neurons are affected, cell death often follows precise patterns that recapitulate the subdivision of these neurons into metabolically and molecularly defined subgroups (14-16). Moreover, in cerebellar mutants, PC death can take different forms, exhibiting mixed features of apoptosis, necrosis and autophagy. For instance, in Lurcher, a gain-of-function mutation for the delta 2 glutamate receptor (17), PC death occurs through different cellular processes (18, 19), including autophagy, by way of molecular interactions between Grid2 and Beclin via n-Pist2 (20).

One of the questions remaining to be addressed in the field is the transcriptional regulation of neuronal survival. Not only is this relevant to our understanding of normal neural development, but it would assist us in dissecting the nature of repair processes that are reactivated or repressed in response to noxious stimuli. Our group and others have analyzed the roles of Collier/Olf/Ebf genes (COE) transcription factors (TFs) in neural development. Ebf genes (reviewed in 21), encode helix-loop-helix (HLH) TFs highly conserved in evolution, that were

originally characterized for their roles in the immune system (22), and subsequently implicated in various aspects of neural development, including neuronal differentiation (23, 24), migration (25, 26), and axon fasciculation and guidance (27-29). One member of this family, *Ebf2*, plays relevant roles in neuroendocrine, olfactory, and peripheral nerve development (30, 31). We and others have shown that EBF2 is important for cerebellar cortical patterning (32, 33) and for PC survival (32). On postnatal day 1, *Ebf2* null mutants lose 38% of their PCs, due to apoptotic cell death (32). This observation prompted us to search for EBF2 targets involved in PC survival during postnatal development, focusing on those coexpressed with *Ebf2* in the cerebellum.

Abundant evidence supports a role for IGF1 and IGF2 in central nervous system (CNS) development. IGF1 is predominantly expressed in neurons in a fashion that coincides with outbursts of neuron progenitor proliferation and/or neurite outgrowth. In contrast, IGF2 expression becomes confined mainly to cells of mesenchymal and neural crest origin. IGF1R is broadly expressed, while IGF binding proteins are regionally and developmentally restricted, correlating with peaks of IGF1 expression (reviewed in 34). In the rodent cerebellum, PCs are the main expression site of IGF1, starting around birth and declining at about P20, to continue throughout adulthood (35, 36) and transgenic overexpression of Igf1 has been shown to promote cerebellar cell survival (37).

In the present paper, we identify Igf1 as a potential transcriptional target of EBF2 using a computer-based prediction approach of EBF target site-containing genes. We show that a subset of *Ebf2* positive PCs expresses the insulin-like growth factor 1 (*Igf1*) gene, and that *Igf1* expression is profoundly downregulated in *Ebf2* null PCs, which die by classical apoptosis. Furthermore, the IGF1/PI3K signaling pathway is downregulated in *Ebf2* null cerebella at birth, and the addition of an IGF1 inhibitor triggers PC death in wt slices at the same stage, while the addition of recombinant IGF1 to *Ebf2* null organotypic cultures rescues PC cell death. Our results reveal that IGF1 is strictly required for PC survival at birth, and shed new light on the local control of *Igf1* gene expression in neurons. This may have farther-reaching implications for the study of molecular mechanisms regulating neuronal survival and neuronal degeneration.

RESULTS

Ebf2 null PCs die by apoptosis within 24 hours of birth. In a previous report we showed that, during postnatal day 1, *Ebf2* null cerebella feature a marked increase in the number of presumptive apoptotic bodies positive for activated caspase 3 (AC3) in the PC layer, particularly in the anterior lobe, that harbors mainly *Ebf2*-positive, zebrinII-negative PCs (32). At this stage, AC3 staining in the PC layer colocalizes with the PC-specific markers retinoic acid-related orphan receptor alpha (Rorα) (**Fig. 1A-C**) or calbindin (CaBP) (Fig. 1D and 32). PC death in the cerebellum has been described extensively using wild type (wt) and mutant animal models, and follows at least three different avenues: necrosis, classical apoptosis and dysregulated autophagy (reviewed in 16).

To better define the type of cell death affecting *Ebf2* null PCs, we analyzed mutant and wt at postnatal day 0.5 (P0.5) cerebella by a combination of approaches: at first, we applied terminal deoxynucleotidyl transferase dUTP nick-end labeling (TUNEL) staining (38), which detects nuclear DNA fragmentation. TUNEL positive cells in the cerebellum were counted as described in Materials and Methods. Our results indicate that, during the first postnatal day, both wt and null cerebella feature a relevant and equivalent degree of TUNEL positivity (p=0.51, Student's *t-test*) in the external granular layer (EGL). However, only mutant cerebella display a high number of TUNEL-positive nuclei in the PC layer (p<0.001) (arrows in **Fig. 1F,H, supplemental Fig. 1D**). The mutant cerebellum also features a significant increase in cell death (p<0.01) in the prospective internal granule layer (IGL) and white matter (WM), which, at this stage, hosts late migrating PCs (CaBP+)(32), oligodendrocyte progenitors (Olig2+) (39), GABA interneurons (Pax2+)(40), few early migrating granule cells and unipolar brush cells (both Pax6+) (41, 42). By immunofluorescence (IF), we found that the majority of the apoptotic bodies are positive for CaBP (as previously shown by 32) (**Fig. 1D,** arrows), while only a low percentage expresses Pax2, Pax6 or Olig2 (**Fig. 1I-K,** arrows).

To confirm that mutant PCs die by apoptosis, we analyzed *Ebf2* null cerebella by electron microscopy. Our results show that the mutant PC layer contains apoptotic bodies characterized by pycnotic, electron-dense nuclei and condensed cytoplasms (**Fig. 1M,O**). Such cellular phenotypes are not detected in the cerebellum of littermate controls (**Fig. 1L,N**).

Because others have shown that, in wt cerebellar slices and in the wt cerebellum, PC death occurs principally between E15 and P6 (reviewed in 16, 43-46), we analyzed the cerebellum of *Ebf2* nulls and control littermates at E19.5 (**supplemental Fig. 1A-D**), P3 (**supplemental Fig.**

1E-H) and P7 (not shown). Our results clearly indicate that the frequency of AC3 and TUNEL positive PCs in *Ebf2* null cerebella is comparable to wt levels at all these stages, while it is increased severely and selectively during the first postnatal day.

Identification of Igf1 as a candidate EBF2 target gene - In the newborn cerebellum, *Ebf2*, as shown by β–galactosidase immunofluorescence in *Ebf2*$^{+/LacZ}$ mice (30), is expressed specifically in Purkinje neurons, where it colocalizes with CaBP (**Fig. 2A,B**). Because EBF2 is a transcription factor (TF) (47, 48), we interrogated sequence databases for genes carrying putative EBF target site(s) (22, 49, 50) in their 5' flanking region, and encoding factors implicated in survival. To this end, we used the Targetfinder software (51). One potentially interesting mediator identified in this way was *Igf1*, a gene encoding a secreted survival factor (34). An evolutionary analysis of the *Igf1* gene promoter (52) revealed that two putative EBF binding sites lie in a highly conserved promoter region (**supplemental Fig. 2**) (*EBF-A* and *EBF-B*, see Materials and methods). In particular, one of the two sites (*EBF-B*) is conserved from mouse to human.

Based on the above evidence, we compared the expression of EBF2 and IGF1 in the cerebellum. At the transcript level, *Ebf2* and *Igf1* colocalize in PCs at E19.5 (**supplemental Fig. 3**) and P0.5 (**Fig. 2C**). To determine whether the IGF1 protein is also expressed in PCs, we performed immunofluorescence staining using IGF1 and CaBP antisera. Our results show that a large number of PCs express IGF1 at birth (**Fig. 2D**, higher magnification in **E**). At the same stage, IGF1 does not appear to be expressed in any other components of the cerebellar cortex, consistent with previously published results (53). This result, together with the one shown in **Fig. 2A,B**, demonstrates that IGF1 and EBF2 are both expressed in neonatal PCs.

Downregulation of Igf1 gene and protein in Ebf2 null PCs. In light of the above findings, we asked if *Igf1* gene expression is downregulated in *Ebf2* null PCs either before or after birth. As shown by *in situ* hybridization, *Igf1* transcript levels are sharply decreased in null PCs at both stages (**Fig. 3B,D**) [FOR THE REVIEWERS: NO *Ebf2* TRANSCRIPT IS DETECTED IN EBF2 NULL CEREBELLA, SEE ATTACHED SUPPLEMENTAL FIGURE REVONLY1]. We also analyzed protein lysates from wt and *Ebf2* null cerebella (n=3 per genotype). A representative western blot is shown in **Fig. 3E**. Results were quantitated and are plotted in **Fig. 3F**. Taken together, these results indicate that, in *Ebf2* null cerebella, IGF1 is downregulated both at the transcript and protein level.

EBF2 regulates Igf1 gene expression in cultured neural cell lines. Subsequently, we sought to confirm the potential transcriptional regulation of *Igf1* expression by EBF2. To this end, we

moved to cultured P19 cells, a multipotent mouse embryo-derived teratocarcinoma cell line. These cells, upon all-trans retinoic acid (RA) treatment, neuralize (54) and activate *Ebf2* expression (G.M. and G.G.C., unpublished results). By reverse transcription-quantitative polymerase chain reaction (RT-qPCR), we analyzed *Igf1* expression after RNAi-mediated knock-down of EBF2 (**Fig. 4C**) using a triple shRNA complementary to the *Ebf2* mRNA at three different sites. The efficiency of this RNAi vector was first validated in *Ebf2*-overexpressing HEK-293 cells (**Fig. 4A,B**). The experiment was then conducted in neuralized P19 cells, that express endogenous *Ebf2* (**Fig. 4C**). Our results show that *Igf1* transcript levels are decreased in P19 cells after *Ebf2* knock-down, 36, 48 and 60 hours post transfection (**Fig. 4D**).

Likewise, we produced a gain of EBF2 function by lipofecting RA treated P19 cells with an *Ebf2*-expressing vector. After 24 hours, *Igf1* expression was analyzed by RT-qPCR. In comparison with mock-transfected cells, *Ebf2* transfected cells showed a 4-fold increase in *Igf1* transcript concentration (**Fig. 4E**). Our results indicate that the effect of EBF2 on *Igf1* gene expression is not restricted to PCs. Thus, in principle, this interaction could be relevant for other *Ebf2*-expressing neural cell types, both during development and in the adult brain.

EBF2 interacts with the Igf1 gene promoter. Next, we asked if EBF2 could regulate *Igf1* gene expression by transcriptional mechanisms. Promoter – reporter gene experiments were performed with COS-7 cells co-transfected with an expression plasmid encoding FLAG-tagged EBF2, and one of three rat *Igf1* promoter 1 – luciferase reporter plasmids containing different 5' truncations of the promoter, and all extending to position +328 that spans the untranslated region of exon 1 (55) (see **Fig. 5A**). The increase in luciferase activity with EBF2 expression was significantly greater with the construct beginning at position -1711 compared to those beginning at positions -823 and -122 (4.5-fold vs. 2.6- and 2.0-fold, respectively), consistent with the presence of at least one EBF response element in the -1711 to -823 segment (**Fig. 5A**). As mentioned, inspection of the nucleotide sequence of the region between -1711 and -823 of rat *Igf1* promoter 1 revealed two putative target sites, (EBF-A and B), in close proximity to one another, and beginning at positions -1106 and -1053 relative to the transcriptional start site.

We used the electrophoretic mobility shift assay (EMSA) to determine if EBF2 could bind directly to either EBF binding site of rat *Igf1* promoter 1. **Fig. 5B** shows results obtained using labeled double-stranded oligonucleotides for each DNA sequence, and nuclear protein extracts from COS-7 cells transfected with expression plasmids for either FLAG-tagged EBF2 or Stat5b, an established *Igf1* transactivator (56). As seen in the figure, nuclear proteins containing EBF2 were able to bind to each DNA element, while those expressing Stat5b were not. Competition experiments with unlabeled homologous DNAs showed specificity of binding, and inhibition of

binding with a known EBF target site from the OcNC promoter (57) provided further support that EBF2 interacts directly with the two elements from *Igf1* promoter 1. In addition, antibody super-shift studies confirmed that EBF2 binds to each oligonucleotide probe.

The *Igf1* gene, consisting of 6 exons and 5 introns, is alternatively spliced in different tissues. Different splicing isoforms at the level of the first coding exon are generated in the liver (exon 2, liver-secreted isoform) vs. other tissues (exon 1, autocrine/paracrine isoform). These isoforms give rise to alternative leader peptides; additional variability is found at the level of exons 4-6, depending on whether or not exon 5 is included in the mature transcript, producing differences in the protein's C-terminus (58). To determine what splicing isoforms of *Igf1* are expressed in the newborn cerebellum, we looked at mRNAs extracted from the wt and mutant. Our results indicate that the prevalent cerebellar isoform contains exon 1 and excludes exons 2 and 5 (**supplemental Fig. 4**). This isoform is underrepresented in the mutant cerebellum. Exon 1 of *Igf1* is located downstream of the EBF2 binding sites identified in the rat promoter, consistent with the finding that EBF2 drives the expression of *Igf1* in the late embryonic and newborn cerebellum.

PI3K signaling pathway downregulation in Ebf2 null PCs - The biological functions of IGF1 are mediated through the type I IGF receptor (IGF1R), a surface receptor tyrosine kinase glycoprotein (59). Upon IGF1 binding, IGF1R is activated by intermolecular autophosphorylation at four sites within the kinase activation loop (60), and phosphorylates the insulin receptor substrates (IRS1-4). This, in turn, leads to mitogen-activated protein kinase (MAPK) and phosphatidylinositol 3-kinase (PI3K) activation (61, 62). In the latter pathway, Ser473 and Thr308 of protein kinase B (PKB/AKT) are sequentially phosphorylated, leading to AKT activation. The PI3K/AKT pathway, is a powerful survival signaling pathway (63). In turn, AKT phosphorylates two pro-apoptotic factors: the BCL2 homolog BAD and the serine kinase GSK3β, inactivating them and promoting cell survival (64-66).

In the newborn cerebellum, an IGF1/PI3K effector, p-AKT^{Ser473}, colocalizes with CaBP expression in PCs, particularly in the anterior lobe (**Fig. 6A,B**). Unlike IGF1, its predominant subcellular localization is in PC dendrites, as previously described (67). We examined the effects of *Ebf2* nullisomy and *Igf1* downregulation on the PI3K pathway in neonatal cerebella. Cerebellar lysates from wt and *Ebf2* null mutants were analyzed by Western blotting with antibodies specific for AKT signaling pathway proteins.

Our results (representative western blots in **Fig. 6C,** quantitation plotted in **D**) indicate that even though total IGF1R and AKT levels are unchanged in null cerebellar lysates, the amounts of p-

AKT^{Thr308} and p-AKT^{Ser473} are significantly reduced. Likewise, p-GSK3β^{Ser9} levels (63) were obviously decreased in the mutant. This result shows that the degree of *Igf1* downregulation observed in our mutants is sufficient to inhibit IGF1R/AKT signal transduction.

IGF1 depletion induces PC apoptosis in wt organotypic tissue culture. Taken together, the above evidence indicates that, in *Ebf2* null cerebella, PC death is preceded by IGF1 downregulation. The next question was whether IGF1 is required for PC survival at birth. To address this point, we resorted to organotypic cerebellar tissue culture. Sagittal slices were derived from wt E19.5 mouse cerebella and cultured as described in Materials and methods. Slices from an hemicerebellum were treated with H-1356, a synthetic IGF1 analog that acts as a competitive inhibitor on the IGF1 receptor (68, 69). Slices from the contralateral hemicerebellum were with vehicle. After 2 days in vitro, cultures were fixed, immunostained for AC3 and CaBP, and analyzed by confocal microscopy. The number of AC3-CaBP double positive PCs was scored, revealing a highly significant increase in the number of apoptotic PCs in H-1356-treated sections vs. control-treated ones (**Fig. 7A,B**, quantitation plotted in **C**). Our results indicate that IGF1 signal inhibition is sufficient to produce massive PC death in the perinatal cerebellum.

Exogenous IGF1 rescues PC apoptosis in Ebf2 null organotypic slices. Finally, to achieve conclusive evidence that IGF1 is the pro-survival factor missing in the *Ebf2* null mutant cerebellum, we attempted to rescue PC apoptosis in *Ebf2* -/- organotypic slices derived as described above. Mutant and control cerebella were divided in two parts, and each hemicerebellum was treated with vehicle or murine purified IGF1. Again, sections were immunostained for CaBP and AC3 and visualized by confocal microscopy. This analysis revealed that the number of apoptotic bodies in the Ebf2 null PC layer was dramatically reduced by IGF1 addition to the culture medium in comparison to vehicle-treated slices (**Fig. 7D,E,** plotted in **H**). Conversely, IGF1 addition had no significant effect on the baseline levels of PC death scored in wt cerebellar slices (**Fig. 7 F,G,** plotted in **H**).

DISCUSSION

The present study confirms that EBF2 controls neonatal PC survival in vivo and in organotypic slices, and indicates that EBF2 activates *Igf1* expression in various cell lines, interacting with a distal *Igf1* promoter element. In late embryogenesis and at birth, *Ebf2* and *Igf1* colocalize neatly in the PC layer, particularly in the anterior and intermediate lobes, with higher expression levels in the former (**Fig. 2**). Wt organotypic cultures plated just before birth are strictly dependent on IGF1 for PC survival. Death in *Ebf2* null slices is rescued by adding purified IGF1 to the medium. Taken together, these results indicate that the increase in PC apoptosis observed in *Ebf2* null mice is due to the downregulation of *Igf1* expression in mutant Purkinje neurons, and strongly suggest that EBF2 supports PC survival by means of directly promoting *Igf1* expression in these cells. While EBF2 is by no means the only TF regulating *Igf1* expression in the cerebellum (71, 72), it appears to act as a critical regulator of *Igf1* transcription and PC survival at birth.

Why the first postnatal day? Purkinje cells are under a great deal of metabolic stress on postnatal day 1. The massive presence of ribosomes in the cytoplasm of newborn PCs has been established for almost 40 years (73, 74). At this stage, PCs start to develop and remodel their dendritic tree, that will eventually receive thousands of afferents from granule cells (75). Furthermore, they elaborate exisiting synaptic contacts with olivocerebellar climbing fibers and begin to establish their first efferent synaptic contacts with deep nuclear neurons (76). Further evidence of the increased susceptibility of PCs at birth came from experiments conducted on cerebellar organotypic slices, revealing that these cells go through a critical period between P1 and P7 (77, 78). Conceivably, PCs at birth require trophic support to sustain this transition, and provide it as an autocrine/paracrine signal through IGF1 secretion.

Why the anterior lobe? Our results raise questions as to why PC death at birth is mostly clustered in the anterior lobe. It is well established that, although all PCs share common morphological features, they are in fact subdivided into several molecularly defined sub-classes arranged into alternate zones and stripes (79, 80). The single most important marker of PC subsets is called zebrin II (81). Zebrin II-positive and negative PCs feature different properties with respect to cell survival, both under physiological and pathological conditions (15, 82, 83). *Ebf2* labels zebrin II-negative PCs (32, 33). *Igf1* is expressed in an anterior-to-posterior gradient at birth, colocalizing with *Ebf2*, in agreement with the prevalent distribution of PCs fated to become zebrin II-negative, and may be required selectively for their survival.

Does IGF1 affect PC survival cell-autonomously? Besides PCs (present paper and 32),

other apoptotic cells are found in the prospective IGL/WM of newborn *Ebf2* mutants. This layer contains a small quota of postmigratory granule cells, numerous UBCs, many GABA interneurons and their progenitors, and oligodendrocyte precursors. Dying cells belong to each of these classes, with a prevalence of PCs delayed in their developmental migration. PC death may possibly stem from the failure of a complex non-cell-autonomous feedback mechanism, whereby PC-secreted IGF1 provides trophic support to other cells which, in turn, protect PCs from apoptosis. However, this is an extremely unlikely scenario, since PC apoptosis only occurs at birth and is complete in a matter of 24 hours. Thus, the most parsimonious explanation is that PCs die due to a cell-autonomous defect in *Igf1* expression, likely increasing their susceptibility to metabolic stress in the first hours of postnatal life.

While granule cells do contribute to PC development later on (84, 85), other authors have shown that at early postnatal stages these cells do not affect PC survival (62). At any rate, granule cells only account for a small minority of the dying cells observed in the *Ebf2* null prospective internal granular layer.

The importance of a local source of Igf1. There is no significant correlation between serum and cerebrospinal fluid IGF concentrations in normal people and patients with pituitary disorders, suggesting that endocrine IGF ligands might not contribute crucially to IGF signaling in the CNS (70). This observation underlines the importance of local sources of IGF1 expression in the nervous system. While long term administration of supraphysiological amounts of IGF1 can protect PCs in an ataxia model (72), our data lend further support to the idea that local *Igf1* transcription is key to neuronal survival at defined stages of development. Our findings indicate that PC survival in the *Ebf2* null mouse is critically dependent upon the local activation of *Igf1* transcription, in agreement with previous findings (58) (35, 86-91).

Besides the cerebellar defects described here, *Ebf2* null mutants feature an impairment in gonadotropic axis and peripheral nerve development (30). IGF1 has been implicated in Gonadotropic Releasing Hormone (GnRH) neuron development and may control both GnRH release (92) and transcription (93). Moreover, the *Ebf2* null peripheral nerve features a defect in axon fasciculation and myelination (30). Again, published studies implicate IGF1 in Schwann cell (SC) differentiation (94) and survival (95). Further studies will be required to establish whether EBF2 controls GnRH neuron- and peripheral nerve development by promoting *Igf1* gene expression.

The controversial roles of IGF1 in neuronal survival and degeneration. While our results indicate that IGF1 is acutely required to support PC survival at birth, conflicting roles have been

described for IGF1 with respect to neuronal survival and ageing. Genetic evidence indicates that a reduction in insulin/IGF1 signaling (IIS) can increase longevity and delay the onset of protein-aggregation-mediated toxicity in invertebrates and mammals alike. Insulin receptor mutation in *C. elegans* (96) and the fruitfly (97) correlate with lifespan extension in those models. Likewise, mice heterozygous for an IGF1R deletion (98) live significantly longer than wt mice. This apparent paradox can be explained by hypothesizing that each organism has an optimal level of insulin/IGF1 signaling (IIS) that maximizes its reproduction, fitness and longevity, and that IIS levels either higher or lower than the optimal rate interfere with metabolism, causing disease and shortening lifespan (99).

Taken together, these observations emphasize the importance of achieving a fine and balanced regulation of *Igf1* gene expression. Transcriptional control by EBF2 is a novel factor in the homeostatic regulation of IIS. EBF2 and other EBF TFs are expressed at many sites in development and after birth (47, 100). Thus, they may participate in *Igf1* regulation at different stages and CNS locations, in physiology and disease.

MATERIALS AND METHODS

Animal Care. All experiments described in this paper were conducted in agreement with the stipulations of the San Raffaele Scientific Institute Animal Care and Use Committee.

Mouse Genetics. All experiments were carried out on F1 hybrids obtained by crossing Ebf2+/– pure-bred FVB/N (N9) females with Ebf2+/– pure-bred C57BL/6J males (30). All studies were conducted using coisogenic control littermates. This hybrid strain was chosen to obviate the low fertility and poor maternal behavior of C57BL/6J heterozygous mothers.

Tissue preparation. Newborn mice were anesthetized with Avertin (Sigma, St. Louis, MO) and perfused with 0.9% NaCl followed by 4% paraformaldehyde (PFA). Embryos were fixed overnight by immersion in 4% PFA. Fixed tissues were rinsed three times in 1X PBS, cryoprotected in 30% sucrose overnight, embedded in OCT (Bioptica, Milan, Italy), and stored at –80°C, before sectioning on a cryotome (20 μm).

Electron microscopy*.* The samples from saline-perfused pups were fixed for 2 hours (hrs) at 4 °C with 4% paraformaldehyde and 2,5% glutaraldehyde in 125 mM cacodylate buffer, then postfixed (1 hr) with 2% OsO4 in 125 mM cacodylate buffer. Samples were washed and embedded in Epon. Electron microscopy analysis was performed on ultrathin transverse sections made on a Leica Ultracut UCT ultramicrotome, stained with uranyl acetate and lead citrate. Slides were examined in a Leo912 electron microscope.

Organotypic cultures. F1 fetuses from embryonic day 19 were used. Fetuses were obtained by cesarean section from pregnant mice anesthetized with Avertin (Sigma). After killing the mice, brains were dissected out into cold DMEM, and meninges were removed. Cerebellar parasagittal slices (300 μm thick) were cut on a McIlwain tissue chopper and separated gently into cold PBS. The slices were cultured on the membrane of a 30 mm Millipore culture insert (Millicell, Millipore, Billerica, MA; pore size 0.4 μm) in 6 cm culture dishes containing 1 ml of medium composed of 50% basal medium with Earle's salts (Sigma), 25% HBSS (Sigma), 25% horse serum (Euroclone, Milan, Italy), L-glutamine (1 mM, Euroclone), and 5 mg/ml glucose (Sigma) at 37°C in an atmosphere of humidified 5% CO_2 (Gahwiler, 1981, 1988; Stoppini et al., 1991). Tissue slices were left in culture for 2 days before further manipulations and treated immediately in the medium with murine purified IGF1 (100ng/ml, Peprotech, Rocky Hill, NJ), IGF1 peptide competitor (30μM, CYAAPLKPAKSC), as previously described (68, 69), or vehicle (1X PBS).

Immunohistochemistry and TUNEL staining. For dual immunofluorescence, floating cryosections were rinsed three times in 1X PBS, preincubated in 15% fetal bovine serum (FBS), 0.2% triton X-100, 1X PBS and incubated overnight at 4°C with the two primary antibodies. Sections were then washed 6X10 min in 1X PBS and incubated for 2 hrs at room temperature with the two secondary antibodies (Alexa 546 anti-rabbit IgG, 1:1 000, and Alexa 488 anti-goat IgG, 1:1 000). Cerebellar organotypic slices were fixed in 4% PFA for 1 hr at room temperature. After 1X PBS washing, the slices were taken off the Millicell and processed for dual immunofluorescence. The slices were preincubated in 15% goat serum, 0.2% triton X-100, 1X PBS and incubated overnight at 4°C with the first antibody (rabbit anti-active Caspase 3). Sections were then washed 6X10 min in 1X PBS and incubated for 2 hrs at room temperature with the secondary antibody (Alexa 546 anti-rabbit IgG, 1:1 000), the slices were washed 6X10 min in 1X PBS and incubated with the second primary antibody (rabbit anti-calbindin) that was labeled before by using a Zenon Alexa Fluor 488 goat anti-rabbit IgG1 kit (Invitrogen) and counterstained with Hoechst (Sigma). In controls either primary antibody was replaced with normal serum. The slices were mounted in Mowiol (Calbiochem, La Jolla, CA) and analyzed using a Leica confocal microscope. TUNEL assay was performed using ApopTag kit (Millipore) according to the manufacturer's instructions. Primary antibodies were as follows: rabbit anti-active Caspase 3, 1:300 (BD Pharmingen, San Jose, CA); goat anti-Rorα, 1:100 (Santa Cruz Biotechnology, Santa Cruz, CA); rabbit anti-Calbindin, 1:1 000 (Swant, Bellinzona, Switzerland); rabbit anti-βgalactosidase, 1:10 000 (Cappel, Costa Mesa, CA); goat anti-IGF1, 1:100 (R&D Systems, Minneapolis, MN); rabbit anti-p-AKT^{Ser473}, 1:50 (Cell Signaling Technology, Danvers, MA). The signal from anti-βgalactosidase, anti-IGF1 and anti-p-AKT^{Ser473} primary antibodies was amplified using the Tyramide Signal Amplification Kit (Perkin Elmer, Waltham, MS).

Cell counts in cryotome sections - The quantitation of TUNEL- and AC3-positive cells (Fig. 1) was obtained counting complete series of sections from wt and mutant P0 cerebella (n=3). Statistical analysis of mean cell numbers and standard deviations in wt versus null mutant sections was conducted using a two-tailed *t-test*, equal variance. On average, TUNEL staining revealed ~15% more unequivocally positive cells than AC3 immunostaining in both wild type and mutant cerebella.

In situ hybridization. Digoxygenin-labeled riboprobes were transcribed from plasmids containing *Ebf2*, *Igf1* and *Rorα* (a gift of B. A. Hamilton) cDNAs. *In situ* hybridizations were performed as described by Pringle and Richardson (http://www.ucl.ac.uk/~ucbzwdr/Richardson.htm). Briefly, the sections were permeabilized with proteinase K (0.5 μg/ml, 7 min), post-fixed with 4% paraformaldehyde, rinsed three times in 1X

PBS, and hybridized with riboprobes in 50% formamide, 3X SSC, 10% dextran sulfate, and 500 μg/ml tRNA solution at 56°C overnight. The sections were washed twice in 50% formamide/2X SSC, treated with Ribonuclease A (20 μg/ml, 30 min), washed in 50% formamide/1X SSC, rinsed in 2X SSC, and incubated with an anti- digoxigenin alkaline phosphatase-conjugated antibody at 4°C overnight. After incubation, the sections were washed three times in 100 mM Tris-HCl (pH 7.5), 150 mM NaCl, then once in 100 mM NaCl, 100 mM Tris-HCl, pH 9.5, 50 mM $MgCl_2$. For a color development reaction, 4-nitroblue tetrazolium chloride (NBT) and 5-bromo-4-chloro-3-indolyl phosphate (BCIP) were used as substrates.

Cell Culture and DNA Transfection. The P19 cell line was maintained in MEM-alpha (Invitrogen) supplemented with 10% FBS (Invitrogen). HEK-293 and COS-7 cell lines were maintained in Dulbecco's modified Eagle's medium (DMEM) supplemented with 10% fetal FBS (EuroClone). P19 and HEK-293 cells were transfected with Lipofectamine2000 (Invitrogen,), and COS-7 with Transit-LT1 (Mirus, Madison, WI) according to protocols of the manufacturers. Depending on the experiment, P19 cells were grown in 5% FBS and 10^{-6} M all-trans retinoic acid (RA, Sigma) for 24, 36, 48, 60 hrs after transfection and sorted for GFP to study shRNA-enriched population. pcDNA3-Flag-Ebf2 construct was a gift from Matthias Kieslinger (University of Munich). pcDNA3 vector, used as a control, was from Clontech (Mountain view, CA).

RNA Interference. Single-stranded DNA oligos encoding the pre-miRNAs were annealed according to the manufacturer's instructions (Invitrogen). Pre-miRNA double-stranded oligos were ligated into pcDNA^{TM}6.2-GW/-EmGFP-miR vector (Invitrogen), that contains a *EGFP* gene. A Pre-miRNA containing a non-targeting sequence (Invitrogen) was used as a negative control. These miRNA vectors were a gift from Matthias Kiesslinger. miRNA targets against *Ebf2* were designed using the BLOCK-iT RNAi designer. Three oligos matching three different sites of the *Ebf2* mRNA were selected in order to maximise knockdown efficiency. This triple miRNA may cross-react with two other members of the Ebf gene family. The three miRNAs were cloned sequentially in the 3'UTR of the *GFP* gene, according to supplier's instructions. The triple shRNA was transfected via Lipofectamine2000 (Invitrogen) according to manufacturer's recommendations. Transfected P19 cells were neuralized with RA (Sigma), then sorted for GFP expression at different time-points and lysed for RNA extraction with RNeasy MiniKit Plus (Qiagen, Valencia, CA), according to manufacturer's instructions.

Reverse Transcription (RT)-PCR Assay. Total RNA was extracted with RNeasy MiniKit Plus (Qiagen), according to the manufacturer's instructions. 1-1,5 μg of total RNA was retro-transcribed using first strand cDNA MMLV-Retrotranscriptase (Invitrogen) and random primers. Each cDNA was diluted 1:10, and 3 μl were used for each reaction. mRNA quantization was

performed using the LightCycler480 SYBR Green I Master Mix (Roche, Mannheim, Germany) on a LighCycler480 instrument (Roche). The following oligonucleotide primers were used: Gapdh (101), Ebf2 TaqMan® probe (Applied Biosystem, Foster City, CA) and *Igf1* (Igf1-F: 5'-GGAGACTGGAGATGTACTGTG; Igf1-R: 5'-GTACTTCCTTCTGAGTCTTGG). Gapdh-F: 5'-TGAAGCAGGCATCTGAGGG; Gapdh-R: 5'- CGAAGGTGGAAGAGTGGGAG. Each gene was analyzed in triplicate, and each experiment was repeated at least three times. Data analysis was performed with the ΔΔCt method (102). All RNA levels were normalized based upon GAPDH transcript levels. For semi-quantitative RT-PCR the following oligonucleotide primers were used: Igf1-Ex1-F: 5'-TCTGCCTCTGTGACTTCTTG; Igf1-Ex2-F: 5'-TCTGACCTGCTGTGTAAACG; Igf1-Ex4-F: 5'-GTTGCTTCCGGAGCTGTGAT; Igf1-Ex4-R: 5'-ATCACAGCTCCGGAAGCAAC; Igf1-Ex6-R: 5'-GGTAGGTGTTTCGATGTTTTG; Hprt-F: 5'-TCCCTGGTTAAGCAGTACAG; Hprt-R: 5'-GACGCAGCAACTGACATTTC.

Electrophoretic mobility shift assays. Electrophoretic mobility shift assays (EMSA) were performed as described (56, 103) with 2.5 μg of COS-7 nuclear proteins prepared from cells transfected with an expression plasmid for FLAG-epitope tagged EBF2 or for FLAG-Stat5b (negative control), and 5'-labeled infrared (IR) double-stranded oligonucleotide probes from putative EBF binding sites in rat IGF1 gene promoter 1, IGF EBF-A from -1110 to -1087 with respect to the most 5' transcription start site (55): top strand, 5'-TCAAATCCCCCGGGAGTGGAGAGT-3', and IGF EBF-B from -1058 to -1037: top strand, 5'-TCCATCTCCCCTGGGAAAGCACT-3' with consensus sites underlined. After incubation of proteins and DNA for 60 min at 4°C, products were separated by electrophoresis through non-denaturing, 5% polyacrylamide gels in 0.5X TBE (45 mM Tris, 45 mM boric acid, and 1 mM EDTA, pH 8.3) at 130 V for 0.5 hr at 20°C. Results were detected using an infrared imager (LiCoR Odyssey), and v3.0 analysis software (LiCoR Biosciences, Lincoln, NB). Antibody super-shift and competition experiments were performed as described (56, 103). The top strand of each heterologous competitor oligonucleotide is as follows: EBF target, OcNC (57): 5'-AAGGGAGAGTCCCTAGGG AGCTTGGGAGGGGCCA-3', Oct-1: 5'-TTTTAGAGGATCCATGCAAATGGACGTACG-3' (Woelfle, J., Billiard, J. and Rotwein, P. (2003) *J Biol Chem* **278**, 22696-22702). Antibodies (1 μg added per lane) were directed against FLAG M2 (Sigma) and T7 epitopes (Novagen, Darmstadt, Germany).

Luciferase assays. COS-7 cells were co-transfected with an expression plasmid for EBF2 or empty vector (pcDNA3), and with one of three promoter-reporter plasmids encoding different segments of rat IGF1 promoter 1 and the entire non-coding region of exon 1, as depicted in Fig 5 (104, 105). After incubation for 40 hrs, cells were harvested and lysates used for luciferase

assays. All results were normalized for total cellular protein values measured by BCA assay (Pierce, Rockford, IL).

Western blotting. HEK-293 cells were harvested 36, 48, 60 and 72 hrs after transfection, and the collected cells were frozen at -80°C. For Western Blots experiments, cells or neonatal cerebellar were lysed in 300 µl of RIPA buffer containing protease inhibitors. Samples were sonicated and centrifuged at 13 000 rpm for 15 minute (min) at 4°C and supernatants collected. Protein concentration was determined by the BCA assay (Pierce). Lysates were mixed with Sample Buffer (125 mM Tris-HCl pH 6.8; 0.1 M 2-mercaptoethanol; 2% SDS; 20% glycerol; 25 mg/ml Bromphenol Blue), boiled for 15 min and separated on an SDS-polyacrylamide gel at 10%. Proteins were transferred on a PVDF membrane (Millipore). Western Blotting were performed with the following antibodies: goat anti-IGF1, 1:100 (R&D Systems), rabbit anti-EBFs, 1: 1 000 (Eurogentec, Liege, Belgium), rabbit anti-IGF1R, 1:1 000 (Cell Signaling Technology), rabbit anti-AKT, 1:1 000 (Cell Signaling Technology), rabbit anti-p-AKT^{Thr308}, 1:500 (Cell Signaling), rabbit anti-p-AKT^{Ser473}, 1:500 (Cell Signaling Technology), rabbit anti-p-GSK3β^{Ser9}, 1:500 (Cell Signaling Technology), mouse anti-βactin, 1:4 000 (Sigma). The secondary antibodies used were a goat anti-rabbit HRP-conjugated antibody, 1:30 000 (Bio-Rad Laboratories, Hercules, CA) and a sheep anti-mouse HRP-conjugated antibody, 1:3 000 (Santa Cruz Biotechnology) and a sheep anti-goat HRP-conjugated antibody, 1:2 000 (DAKO, Glostrup, Denmark). Blots were developed with the LiteAblot substrate (EuroClone).

Statistical Analysis. Statistical significance was determined by the Student *t*-test and Pearson's chi-square test, for the analysis of organotypic data, with a threshold for significance set to $p \leq 0.05$. All data are plotted as the mean ± standard deviation, unless stated otherwise.

ACKNOWLEDGEMENTS

Image analysis was carried out by Maria Carla Panzeri at Alembic, a microscopy laboratory established by the San Raffaele Scientific Institute and Vita-Salute San Raffele University. The authors are grateful to Alessio Palini, San Raffaele Scientific Institute, for his help with cytofluorimetric analysis. We are sincerely grateful to Matthias Kieslinger (Munich) for the gift of mouse Ebf-specific shRNA vectors and Ebf expression vectors. GGC was supported the Italian Ministry of University (MIUR) through FIRB grant RBLA03AF28_002. Additional support to this work came from Fondazione Mariani (Milan) and Italian Ministry of Health grants to GGC.

REFERENCES

1. Putcha GV, Johnson EM, Jr. Men are but worms: neuronal cell death in C elegans and vertebrates. *Cell Death Differ* 2004 Jan; **11**(1)**:** 38-48.

2. Graham A, Francis-West P, Brickell P, Lumsden A. The signalling molecule BMP4 mediates apoptosis in the rhombencephalic neural crest. *Nature* 1994 Dec 15; **372**(6507)**:** 684-686.

3. Zou H, Niswander L. Requirement for BMP signaling in interdigital apoptosis and scale formation. *Science* 1996 May 3; **272**(5262)**:** 738-741.

4. Chen G, Goeddel DV. TNF-R1 signaling: a beautiful pathway. *Science* 2002 May 31; **296**(5573)**:** 1634-1635.

5. Wajant H. The Fas signaling pathway: more than a paradigm. *Science* 2002 May 31; **296**(5573)**:** 1635-1636.

6. Lamborghini JE. Disappearance of Rohon-Beard neurons from the spinal cord of larval Xenopus laevis. *J Comp Neurol* 1987 Oct 1; **264**(1)**:** 47-55.

7. Bernhardt RR, Chitnis AB, Lindamer L, Kuwada JY. Identification of spinal neurons in the embryonic and larval zebrafish. *J Comp Neurol* 1990 Dec 15; **302**(3)**:** 603-616.

8. Yuan JY, Horvitz HR. The Caenorhabditis elegans genes ced-3 and ced-4 act cell autonomously to cause programmed cell death. *Dev Biol* 1990 Mar; **138**(1)**:** 33-41.

9. Cecconi F, Alvarez-Bolado G, Meyer BI, Roth KA, Gruss P. Apaf1 (CED-4 homolog) regulates programmed cell death in mammalian development. *Cell* 1998 Oct 18; **94**(6)**:** 727-737.

10. Zanjani HS, Vogel MW, Delhaye-Bouchaud N, Martinou JC, Mariani J. Increased cerebellar Purkinje cell numbers in mice overexpressing a human bcl-2 transgene. *J Comp Neurol* 1996 Oct 21; **374**(3)**:** 332-341.

11. Snider WD. Functions of the neurotrophins during nervous system development: what the knockouts are teaching us. *Cell* 1994 Jun 3; **77**(5)**:** 627-638.

12. von Bartheld CS, Wang X, Butowt R. Anterograde axonal transport, transcytosis, and recycling of neurotrophic factors: the concept of trophic currencies in neural networks. *Mol Neurobiol* 2001 Aug-Dec; **24**(1-3)**:** 1-28.

13. Huang EJ, Reichardt LF. Neurotrophins: roles in neuronal development and function. *Annu Rev Neurosci* 2001; **24:** 677-736.

14. Wassef M, Sotelo C, Cholley B, Brehier A, Thomasset M. Cerebellar mutations affecting the postnatal survival of Purkinje cells in the mouse disclose a longitudinal pattern of differentially sensitive cells. *Dev Biol* 1987 Dec; **124**(2)**:** 379-389.

15. Sarna J, Miranda SR, Schuchman EH, Hawkes R. Patterned cerebellar Purkinje cell death in a transgenic mouse model of Niemann Pick type A/B disease. *Eur J Neurosci* 2001 May; **13**(10)**:** 1873-1880.

16. Dusart I, Guenet JL, Sotelo C. Purkinje cell death: differences between developmental cell death and neurodegenerative death in mutant mice. *Cerebellum* 2006; **5**(2)**:** 163-173.

17. Zuo J, De Jager PL, Takahashi KA, Jiang W, Linden DJ, Heintz N. Neurodegeneration in Lurcher mice caused by mutation in delta2 glutamate receptor gene. *Nature* 1997 Aug 21; **388**(6644)**:** 769-773.

18. Norman D, Feng L, Cheng S, Gubbay J, Chan E, Heintz N. The lurcher gene induces apoptotic death in cerebellar Purkinje cells. *Development* 1995; **121:** 1183-1193.

19. Doughty ML, De Jager PL, Korsmeyer SJ, Heintz N. Neurodegeneration in Lurcher mice occurs via multiple cell death pathways. *J Neurosci* 2000 May 15; **20**(10)**:** 3687-3694.

20. Yue Z, Horton A, Bravin M, DeJager PL, Selimi F, Heintz N. A novel protein complex linking the delta 2 glutamate receptor and autophagy: implications for neurodegeneration in lurcher mice. *Neuron* 2002 Aug 29; **35**(5)**:** 921-933.

21. Dubois L, Vincent A. The COE--Collier/Olf1/EBF--transcription factors: structural conservation and diversity of developmental functions. *Mech Dev* 2001; **108**(1-2)**:** 3-12.

22. Hagman J, Belanger C, Travis A, Turck C, Grosschedl R. Cloning and functional characterization of early B-cell factor, a regulator of lymphocyte-specific gene expression. *Genes Dev* 1993; **7:** 760-773.

23. Dubois L, Bally-Cuif L, Crozatier M, Moreau J, Paquereau L, Vincent L. XCoe2, a transcription factor of the Col/Olf-1/EBF family involved in the specification of primary neurons in *Xenopus*. *Current Biology* 1998; **8:** 199-209.

24. Pozzoli O, Bosetti A, Croci L, Consalez GG, Vetter ML. Xebf3 is a regulator of neuronal differentiation during primary neurogenesis in Xenopus. *Dev Biol* 2001; **233**(2)**:** 495-512.

25. Garel S, Garcia-Dominiguez M, Charnay P. Control of the migratory pathway of facial branchiomotor neurones. *Development* 2000; **127**(24)**:** 5297-5307.

26. Garcia-Dominguez M, Poquet C, Garel S, Charnay P. Ebf gene function is required for coupling neuronal differentiation and cell cycle exit. *Development* 2003 Dec; **130**(24)**:** 6013-6025.

27. Prasad BC, Ye B, Zackhary R, Schrader K, Seydoux G, Reed RR. unc-3, a gene required for axonal guidance in Caenorhabditis elegans, encodes a member of the O/E family of transcription factors. *Development* 1998; **125**(8)**:** 1561-1568.

28. Garel S, Yun K, Grosschedl R, Rubenstein JL. The early topography of thalamocortical projections is shifted in Ebf1 and Dlx1/2 mutant mice. *Development* 2002; **129**(24)**:** 5621-5634.

29. Garel S, Marin F, Grosscheld R, Charnay P. Ebf1 controls early cell differentiation in the embryonic striatum. *Development* 1999; **126**(23)**:** 5285-5294.

30. Corradi A, Croci L, Broccoli V, Zecchini S, Previtali S, Wurst W*, et al.* Hypogonadotropic hypogonadism and peripheral neuropathy in Ebf2-null mice. *Development* 2003 Jan; **130**(2)**:** 401-410.

31. Wang SS, Lewcock JW, Feinstein P, Mombaerts P, Reed RR. Genetic disruptions of O/E2 and O/E3 genes reveal involvement in olfactory receptor neuron projection. *Development* 2004 Mar; **131**(6)**:** 1377-1388.

32. Croci L, Chung SH, Masserdotti G, Gianola S, Bizzoca A, Gennarini G*, et al.* A key role for the HLH transcription factor EBF2COE2,O/E-3 in Purkinje neuron migration and cerebellar cortical topography. *Development* 2006 Jul; **133**(14)**:** 2719-2729.

33. Chung S-H, Marzban H, Croci L, Consalez G, Hawkes R. Purkinje cell subtype specification in the cerebellar cortex: Ebf2 acts to repress the Zebrin II-positive Purkinje cell phenotype. *Neuroscience* 2008; **153:** 721-732.

34. D'Ercole AJ, Ye P, Calikoglu AS, Gutierrez-Ospina G. The role of the insulin-like growth factors in the central nervous system. *Mol Neurobiol* 1996 Dec; **13**(3)**:** 227-255.

35. Aguado F, Sanchez-Franco F, Rodrigo J, Cacicedo L, Martinez-Murillo R. Insulin-like growth factor I-immunoreactive peptide in adult human cerebellar Purkinje cells: co-localization with low-affinity nerve growth factor receptor. *Neuroscience* 1994; **59**(3)**:** 641-650.

36. Torres-Aleman I, Pons S, Arevalo MA. The insulin-like growth factor I system in the rat cerebellum: developmental regulation and role in neuronal survival and differentiation. *J Neurosci Res* 1994 Oct 1; **39**(2)**:** 117-126.

37. Chrysis D, Calikoglu AS, Ye P, D'Ercole AJ. Insulin-like growth factor-I overexpression attenuates cerebellar apoptosis by altering the expression of Bcl family proteins in a developmentally specific manner. *J Neurosci* 2001 Mar 1; **21**(5)**:** 1481-1489.

38. Gavrieli Y, Sherman Y, Ben-Sasson SA. Identification of programmed cell death in situ via specific labeling of nuclear DNA fragmentation. *J Cell Biol* 1992 Nov; **119**(3)**:** 493-501.

39. Grimaldi P, Parras C, Guillemot F, Rossi F, Wassef M. Origins and control of the differentiation of inhibitory interneurons and glia in the cerebellum. *Dev Biol* 2009 Apr 15; **328**(2)**:** 422-433.

40. Leto K, Carletti B, Williams IM, Magrassi L, Rossi F. Different types of cerebellar GABAergic interneurons originate from a common pool of multipotent progenitor cells. *J Neurosci* 2006 Nov 8; **26**(45)**:** 11682-11694.

41. Karam SD, Kim YS, Bothwell M. Granule cells migrate within raphes in the developing cerebellum: an evolutionarily conserved morphogenic event. *J Comp Neurol* 2001 Nov 12; **440**(2)**:** 127-135.

42. Englund C, Kowalczyk T, Daza RA, Dagan A, Lau C, Rose MF*, et al.* Unipolar brush cells of the cerebellum are produced in the rhombic lip and migrate through developing white matter. *J Neurosci* 2006 Sep 6; **26**(36)**:** 9184-9195.

43. Ghoumari AM, Wehrle R, De Zeeuw CI, Sotelo C, Dusart I. Inhibition of protein kinase C prevents Purkinje cell death but does not affect axonal regeneration. *J Neurosci* 2002 May 1; **22**(9)**:** 3531-3542.

44. Kitao Y, Hashimoto K, Matsuyama T, Iso H, Tamatani T, Hori O*, et al.* ORP150/HSP12A regulates Purkinje cell survival: a role for endoplasmic reticulum stress in cerebellar development. *J Neurosci* 2004 Feb 11; **24**(6)**:** 1486-1496.

45. Marin-Teva JL, Dusart I, Colin C, Gervais A, van Rooijen N, Mallat M. Microglia promote the death of developing Purkinje cells. *Neuron* 2004 Feb 19; **41**(4)**:** 535-547.

46. Goswami J, Martin LA, Goldowitz D, Beitz AJ, Feddersen RM. Enhanced Purkinje cell survival but compromised cerebellar function in targeted anti-apoptotic protein transgenic mice. *Mol Cell Neurosci* 2005 Jun; **29**(2)**:** 202-221.

47. Malgaretti N, Pozzoli O, Bosetti A, Corradi A, Ciarmatori S, Panigada M*, et al.* Mmot1, a new helix-loop-helix transcription factor gene displaying a sharp expression boundary in the embryonic mouse brain. *J Biol Chem* 1997 Jul 11; **272**(28)**:** 17632-17639.

48. Wang SS, Tsai RYL, Reed RR. The characterization of the Olf-1/EBF-like HLH transcription factor family: implications in olfactory gene regulation and neuronal development. *J Neurosci* 1997; **17:** 4149-4158.

49. Kudrycki K, Stein-Izsak C, Behn C, Grillo M, Akeson R, Margolis FL*, et al.* Olf-1-binding site: characterization of an olfactory neuron-specific promoter motif. *Molecular & Cellular Biology* 1993; **13**(5)**:** 3002-3014.

50. Travis A, Hagman J, Hwang L, Grosschedl R. Purification of early-B-cell factor and characterization of its DNA-binding specificity. *Molecular & Cellular Biology* 1993; **13**(6)**:** 3392-3400.

51. Lavorgna G, Guffanti A, Borsani G, Ballabio A, Boncinelli E. Targetfinder: to search annotated sequence databases for target genes of transcription factors. *Bioinformatics* 1999; **15:** 172-173.

52. Ovcharenko I, Nobrega MA, Loots GG, Stubbs L. ECR Browser: a tool for visualizing and accessing data from comparisons of multiple vertebrate genomes. *Nucleic Acids Res* 2004 Jul 1; **32**(Web Server issue)**:** W280-286.

53. Bondy CA. Transient IGF-I gene expression during the maturation of functionally related central projection neurons. *J Neurosci* 1991 Nov; **11**(11)**:** 3442-3455.

54. Jones-Villeneuve EM, McBurney MW, Rogers KA, Kalnins VI. Retinoic acid induces embryonal carcinoma cells to differentiate into neurons and glial cells. *J Cell Biol* 1982 Aug; **94**(2)**:** 253-262.

55. Hall LJ, Kajimoto Y, Bichell D, Kim SW, James PL, Counts D*, et al.* Functional analysis of the rat insulin-like growth factor I gene and identification of an IGF-I gene promoter. *DNA and cell biology* 1992 May; **11**(4)**:** 301-313.

56. Woelfle J, Billiard J, Rotwein P. Acute control of insulin-like growth factor-I gene transcription by growth hormone through Stat5b. *J Biol Chem* 2003 Jun 20; **278**(25)**:** 22696-22702.

57. Baumeister H, Gronostajski RM, Lyons GE, Margolis FL. Identification of NFI-binding sites and cloning of NFI-cDNAs suggest a regulatory role for NFI transcription factors in olfactory neuron gene expression. *Brain Res Mol Brain Res* 1999 Sep 8; **72**(1)**:** 65-79.

58. Musaro A, Dobrowolny G, Rosenthal N. The neuroprotective effects of a locally acting IGF-1 isoform. *Exp Gerontol* 2007 Jan-Feb; **42**(1-2)**:** 76-80.

59. Kim B, van Golen CM, Feldman EL. Insulin-like growth factor-I signaling in human neuroblastoma cells. *Oncogene* 2004 Jan 8; **23**(1)**:** 130-141.

60. Favelyukis S, Till JH, Hubbard SR, Miller WT. Structure and autoregulation of the insulin-like growth factor 1 receptor kinase. *Nat Struct Biol* 2001 Dec; **8**(12)**:** 1058-1063.

61. Torres-Aleman I, Villalba M, Nieto-Bona MP. Insulin-like growth factor-I modulation of cerebellar cell populations is developmentally stage-dependent and mediated by specific intracellular pathways. *Neuroscience* 1998 Mar; **83**(2)**:** 321-334.

62. Fukudome Y, Tabata T, Miyoshi T, Haruki S, Araishi K, Sawada S*, et al.* Insulin-like growth factor-I as a promoting factor for cerebellar Purkinje cell development. *Eur J Neurosci* 2003 May; **17**(10)**:** 2006-2016.

63. Bondy CA, Cheng CM. Signaling by insulin-like growth factor 1 in brain. *Eur J Pharmacol* 2004 Apr 19; **490**(1-3)**:** 25-31.

64. Prisco M, Romano G, Peruzzi F, Valentinis B, Baserga R. Insulin and IGF-I receptors signaling in protection from apoptosis. *Hormone and metabolic research Hormon- und Stoffwechselforschung* 1999 Feb-Mar; **31**(2-3)**:** 80-89.

65. Hetman M, Cavanaugh JE, Kimelman D, Xia Z. Role of glycogen synthase kinase-3beta in neuronal apoptosis induced by trophic withdrawal. *J Neurosci* 2000 Apr 1; **20**(7)**:** 2567-2574.

66. Cross DA, Alessi DR, Cohen P, Andjelkovich M, Hemmings BA. Inhibition of glycogen synthase kinase-3 by insulin mediated by protein kinase B. *Nature* 1995 Dec 21-28; **378**(6559)**:** 785-789.

67. Cheng CM, Reinhardt RR, Lee WH, Joncas G, Patel SC, Bondy CA. Insulin-like growth factor 1 regulates developing brain glucose metabolism. *Proc Natl Acad Sci U S A* 2000 Aug 29; **97**(18)**:** 10236-10241.

68. Pietrzkowski Z, Wernicke D, Porcu P, Jameson BA, Baserga R. Inhibition of cellular proliferation by peptide analogues of insulin-like growth factor 1. *Cancer Res* 1992 Dec 1; **52**(23)**:** 6447-6451.

69. Ozdinler PH, Macklis JD. IGF-I specifically enhances axon outgrowth of corticospinal motor neurons. *Nat Neurosci* 2006 Nov; **9**(11)**:** 1371-1381.

70. Backstrom M, Hall K, Sara V. Somatomedin levels in cerebrospinal fluid from adults with pituitary disorders. *Acta endocrinologica* 1984 Oct; **107**(2)**:** 171-178.

71. Kim BJ, Takamoto N, Yan J, Tsai SY, Tsai MJ. Chicken Ovalbumin Upstream Promoter-Transcription Factor II (COUP-TFII) regulates growth and patterning of the postnatal mouse cerebellum. *Dev Biol* 2008 Nov 14.

72. Bitoun E, Finelli MJ, Oliver PL, Lee S, Davies KE. AF4 is a critical regulator of the IGF-1 signaling pathway during Purkinje cell development. *J Neurosci* 2009 Dec 9; **29**(49)**:** 15366-15374.

73. Nosal G, Radouco-Thomas C. Ultrastructural study on the differentiation and development of the nerve cell: the "nucleus-ribosome" system. *Adv Cytopharmacol* 1971 May; **1:** 433-456.

74. Sotelo C. Viewing the cerebellum through the eyes of Ramon Y Cajal. *Cerebellum* 2008; **7**(4)**:** 517-522.

75. Armengol JA, Sotelo C. Early dendritic development of Purkinje cells in the rat cerebellum. A light and electron microscopic study using axonal tracing in 'in vitro' slices. *Brain Res Dev Brain Res* 1991 Dec 17; **64**(1-2)**:** 95-114.

76. Gardette R, Debono M, Dupont JL, Crepel F. Electrophysiological studies on the postnatal development of intracerebellar nuclei neurons in rat cerebellar slices maintained in vitro. II. Membrane conductances. *Brain Res* 1985 May; **352**(1)**:** 97-106.

77. Dusart I, Airaksinen MS, Sotelo C. Purkinje cell survival and axonal regeneration are age dependent: an in vitro study. *J Neurosci* 1997 May 15; **17**(10)**:** 3710-3726.

78. Ghoumari AM, Wehrle R, Bernard O, Sotelo C, Dusart I. Implication of Bcl-2 and Caspase-3 in age-related Purkinje cell death in murine organotypic culture: an in vitro model to study apoptosis. *Eur J Neurosci* 2000 Aug; **12**(8)**:** 2935-2949.

79. Hawkes R. Antigenic markers of cerebellar modules in the adult mouse. *Biochem Soc Trans* 1992 May; **20**(2)**:** 391-395.

80. Herrup K, Kuemerle B. The compartmentalization of the cerebellum [Review]. *Annual Review of Neuroscience* 1997; **20:** 61-90.

81. Brochu G, Maler L, Hawkes R. Zebrin II: a polypeptide antigen expressed selectively by Purkinje cells reveals compartments in rat and fish cerebellum. *J Comp Neurol* 1990 Jan 22; **291**(4)**:** 538-552.

82. Sarna JR, Hawkes R. Patterned Purkinje cell death in the cerebellum. *Prog Neurobiol* 2003 Aug; **70**(6)**:** 473-507.

83. Sarna JR, Larouche M, Marzban H, Sillitoe RV, Rancourt DE, Hawkes R. Patterned Purkinje cell degeneration in mouse models of Niemann-Pick type C disease. *J Comp Neurol* 2003 Feb 10; **456**(3)**:** 279-291.

84. Crepel F, Delhaye-Bouchaud N, Dupont JL, Sotelo C. Dendritic and axonic fields of Purkinje cells in developing and x-irradiated rat cerebellum. A comparative study using intracellular staining with horseradish peroxidase. *Neuroscience* 1980; **5**(2)**:** 333-347.

85. Sotelo C. Purkinje cell ontogeny: formation and maintenance of spines. *Prog Brain Res* 1978; **48:** 149-170.

86. Heck S, Lezoualc'h F, Engert S, Behl C. Insulin-like growth factor-1-mediated neuroprotection against oxidative stress is associated with activation of nuclear factor kappaB. *J Biol Chem* 1999 Apr 2; **274**(14)**:** 9828-9835.

87. Olson BR, Scott DC, Wetsel WC, Elliot SJ, Tomic M, Stojilkovic S*, et al.* Effects of insulin-like growth factors I and II and insulin on the immortalized hypothalamic GTI-7 cell line. *Neuroendocrinology* 1995 Aug; **62**(2)**:** 155-165.

88. Dore S, Kar S, Quirion R. Insulin-like growth factor I protects and rescues hippocampal neurons against beta-amyloid- and human amylin-induced toxicity. *Proc Natl Acad Sci U S A* 1997 Apr 29; **94**(9)**:** 4772-4777.

89. Niikura T, Hashimoto Y, Okamoto T, Abe Y, Yasukawa T, Kawasumi M*, et al.* Insulin-like growth factor I (IGF-I) protects cells from apoptosis by Alzheimer's V642I mutant amyloid precursor protein through IGF-I receptor in an IGF-binding protein-sensitive manner. *J Neurosci* 2001 Mar 15; **21**(6)**:** 1902-1910.

90. Linseman DA, Phelps RA, Bouchard RJ, Le SS, Laessig TA, McClure ML*, et al.* Insulin-like growth factor-I blocks Bcl-2 interacting mediator of cell death (Bim) induction and intrinsic death signaling in cerebellar granule neurons. *J Neurosci* 2002 Nov 1; **22**(21)**:** 9287-9297.

91. Vig PJ, Subramony SH, D'Souza DR, Wei J, Lopez ME. Intranasal administration of IGF-I improves behavior and Purkinje cell pathology in SCA1 mice. *Brain Res Bull* 2006 May 15; **69**(5)**:** 573-579.

92. Miller BH, Gore AC. Alterations in hypothalamic insulin-like growth factor-I and its associations with gonadotropin releasing hormone neurones during reproductive development and ageing. *J Neuroendocrinol* 2001 Aug; **13**(8)**:** 728-736.

93. Longo KM, Sun Y, Gore AC. Insulin-like growth factor-I effects on gonadotropin-releasing hormone biosynthesis in GT1-7 cells. *Endocrinology* 1998 Mar; **139**(3)**:** 1125-1132.

94. Russell JW, Cheng HL, Golovoy D. Insulin-like growth factor-I promotes myelination of peripheral sensory axons. *J Neuropathol Exp Neurol* 2000 Jul; **59**(7)**:** 575-584.

95. Syroid DE, Zorick TS, Arbet-Engels C, Kilpatrick TJ, Eckhart W, Lemke G. A role for insulin-like growth factor-I in the regulation of Schwann cell survival. *J Neurosci* 1999 Mar 15; **19**(6)**:** 2059-2068.

96. Kimura KD, Tissenbaum HA, Liu Y, Ruvkun G. daf-2, an insulin receptor-like gene that regulates longevity and diapause in Caenorhabditis elegans. *Science* 1997 Aug 15; **277**(5328)**:** 942-946.

97. Tatar M, Kopelman A, Epstein D, Tu MP, Yin CM, Garofalo RS. A mutant Drosophila insulin receptor homolog that extends life-span and impairs neuroendocrine function. *Science* 2001 Apr 6; **292**(5514)**:** 107-110.

98. Holzenberger M, Dupont J, Ducos B, Leneuve P, Geloen A, Even PC*, et al.* IGF-1 receptor regulates lifespan and resistance to oxidative stress in mice. *Nature* 2003 Jan 9; **421**(6919)**:** 182-187.

99. Cohen E, Dillin A. The insulin paradox: aging, proteotoxicity and neurodegeneration. *Nat Rev Neurosci* 2008 Oct; **9**(10)**:** 759-767.

100. Garel S, Marin F, Mattei MG, Vesque C, Vincent A, Charnay P. Family of Ebf/Olf-1-related genes potentially involved in neuronal differentiation and regional specification in the central nervous system. *Dev Dyn* 1997; **210**(3)**:** 191-205.

101. Vincent VA, DeVoss JJ, Ryan HS, Murphy GM, Jr. Analysis of neuronal gene expression with laser capture microdissection. *J Neurosci Res* 2002 Sep 1; **69**(5)**:** 578-586.

102. Livak KJ, Schmittgen TD. Analysis of relative gene expression data using real-time quantitative PCR and the 2(-Delta Delta C(T)) Method. *Methods* 2001 Dec; **25**(4)**:** 402-408.

103. Gronowski AM, Rotwein P. Rapid changes in nuclear protein tyrosine phosphorylation after growth hormone treatment in vivo. Identification of phosphorylated mitogen-activated protein kinase and STAT91. *J Biol Chem* 1994 Mar 18; **269**(11)**:** 7874-7878.

104. Austin KD, Hall JG. Nontraditional inheritance. *Pediatric Clinics of North America* 1992; **39**(2)**:** 335-348.

105. McCarthy TL, Thomas MJ, Centrella M, Rotwein P. Regulation of insulin-like growth factor I transcription by cyclic adenosine 3',5'-monophosphate (cAMP) in fetal rat bone cells through an element within exon 1: protein kinase A-dependent control without a consensus AMP response element. *Endocrinology* 1995 Sep; **136**(9)**:** 3901-3908.

FIGURE LEGENDS

Figure 1 – Ebf2 null PCs die by apoptosis shortly after birth. **A-D,** double immunofluorescence on P0.5 sagittal sections, as labeled. In wild type (wt) mice, cell death, as assessed by activated caspase 3 (AC3) immunoreactivity, is only detectable in the prospective igl/white matter (pwm), not in the PC layer (arrowheads in **A**). In the mutant cerebellum, most apoptotic cells are retinoic acid-related orphan receptor alpha (RORα)-positive PCs (**B**, arrows in **C**). However, dying PCs, positive for calbindin (CaBP), are also found in the mutant pwm (arrows in **D**). **E-H**, TUNEL assay on frontal sections from wt (**E,G**) and null mutant (**F,H**) cerebella. DNA fragmentation (red fluorescent dots) is evident only in the *Ebf2* null PC layer (pcl) (arrows in **F,H**). Note the comparable levels of apoptosis in the external granular layer (egl) of *Ebf2* null vs wt control sections. **I-K**, in the mutant cerebellum only few TUNEL+ cells located in the pwm are positive for Pax2, Pax6 and Olig2 specific markers (arrows). **L-O**, electron microscopy imaging of wt (**L,N**) and *Ebf2* null (**M,O**) PCs. Wt PCs feature large nuclei with round nucleoli (asterisk). Their cytoplasm is rich in polysomes (circled area) and contains intact mitochondria (arrowheads). Conversely, in the mutant cerebellum (**M,O**), numerous apoptotic bodies are found, characterized by a pycnotic nucleus (nc) and condensed cytoplasm (arrow). Scale bar: **A-C**, 200 μm; **D**, 50 μm; **E-H**, 100 μm; **I-K, 20** μm; **L,N,O**, 1 μm; **M**, 2 μm.

Figure 2 – Ebf2 and Igf1 are co-expressed in PCs shortly after birth. **A,** βgal, a reporter of *Ebf2* expression in $Ebf2^{+/LacZ}$ heterozygotes, is preferentially expressed in PCs located in the anterior lobe (**A**, higher magnification in **B**). **C**, *in situ* hybridization on sagittal cerebellar sections hybridized with an *Ebf2* or with an *Igf1* cRNA probe. PCs that express *Igf1* are also positive for *Ebf2* (**C**). **D**, higher magnification in **E**, double immunostaining for CaBP and IGF1 on sagittal cerebellar sections. At both the transcript and protein levels, Ebf2 and IGF1 are found expressed in PCs. pcl: Purkinje cell layer; egl: external granular layer. Scale bar: **A,D**, 500 μm; **B,** 40 μm**; C**, 200 μm; **E,** 20 μm.

Figure 3 - Igf1 expression is downregulated in Ebf2 null PCs. **A-D,** *in situ* hybridization on E19.5 and P0.5 frontal cerebellar sections (sectioning plane sketched at bottom left). In the wt, *Igf1* is detectable in a subset of PCs as revealed by comparing its distribution to that of *Ror*α in adjacent sections. The *Igf1* transcript is almost absent in *Ebf2* null PCs (arrows). **E**, western blot analysis of IGF1 protein

shows a significant reduction in *Ebf2* null lysates compared to the wt (protein levels plotted in **F**). The experiment was repeated on protein extracts from three wt and mutant cerebella with the standard deviation (SD) in each case. pcl: Purkinje cell layer; egl: external granular layer. Scale bar: 200 µm. *p<0,05.

Figure 4 - EBF2 activates Igf1 expression in P19 cells. **A**, To determine whether our *Ebf2*-specific shRNA was effective in downregulating EBF2 protein levels, we overexpressed a flag-tagged *Ebf2* in HEK-293 cells that do not exhibit detectable levels of endogenous *Ebf2.* Western blotting results show that *flag-Ebf2*-overexpressing HEK-293 cells cotransfected with an *Ebf2* shRNA (*Ebf2*-sh) exhibit a complete downregulation of flag-EBF2 protein levels, compared to cells cotransfected with a mock sh-RNA (mock-sh). **B**, quantitative analysis of the experiment described in **A**. Band intensities in sh-treated samples, relative to mock treatment, were measured using the ImageQuant software. All protein levels were also normalized to β-actin. **C**, time course of endogenous *Ebf2* gene expression in neuralized P19 cells after EBF2 knock-down with the *Ebf2*-sh vector (black columns), relative to the corresponding transcript level in cells treated with mock shRNA (empty column). **D**, time course of endogenous *Igf1* gene expression in cells treated as detailed in **C**. **E**, induction of endogenous *Igf1* gene expression in neuralized P19 cells transfected with an *Ebf2* expression vector after 24 hours. **C-E,** SDs are indicated in each histogram. All the experiments shown were repeated three times. *p<0.05; ** p<0.01.

Figure 5 - EBF2 binds two sequences of Igf1 promoter 1 and enhances promoter activity. **A**, results of luciferase assays in COS-7 cells transiently transfected with an expression plasmid for *Ebf2* (or an empty vector) and with the *Igf1* promoter-reporter plasmids, as sketched. The graph summarizes results of four independent experiments (mean +/- S.E.), each performed in duplicate and normalized for total protein content with the SD in each case. The asterisks indicate significant difference in EBF2-induced promoter activity (p<0.03) in comparison to the -1711 promoter-reporter plasmid that spans putative binding sites IGF EBF-A and -B. Basal luciferase values ranged from 10 000 to 135 000 relative light units/10 s. **B**, results of gel-mobility shift assays using IR-labeled double-stranded oligonucleotides for either IGF EBF-A or -B of rat *Igf1* promoter 1. The DS oligos were incubated with nuclear protein extracts from COS-7 cells transfected with expression plasmids encoding FLAG-tagged EBF2 or the unrelated STAT5b. Protein-DNA complexes are observed only with nuclear extracts from EBF2-expressing cells. 50-fold excess of

unlabeled homologous oligonucleotide and a previously described EBF binding site of the *OcNC* gene effectively compete off binding, while an *Oct-1* recognition site does not. A supershift of each protein-DNA complex (asterisk) is seen with an antibody to the FLAG-epitope, but not with the T7 irrelevant antibody directed against the 11 amino acid of the T7 phage gene 10 leader peptide. Unbound probe is observed at the bottom of each gel.

Figure 6 - Reduced AKT1 phosphorylation in the Ebf2 null cerebellum. **A**, P0.5 sagittal sections from an *Ebf2*$^{+/LacZ}$ cerebellum immunostained for CaBP and the IGF1 effector AKT, phosphorylated in Ser^{473}. Phospho-AKT staining in PCs reveals the activation of the IGF1R/PI3K signaling pathway in these cells, specifically in dendrites (arrows in **B**). **C**, cerebellar protein extracts from wt and *Ebf2* null mice were analyzed by western blotting at the same stage (P0.5). The levels of AKT phosporylation at both Ser473 and Thr308, and GSK3b phosporylation at Ser9 are dramatically reduced in *Ebf2* –/– lysates, while total AKT and IGF1R levels are unchanged. **D**, the intensity of immunoreactivity was quantified using the ImageJ software. Protein levels were normalized to β-actin. Each immunoblotting experiment was repeated on protein extracts from four independent wt and null mutant mice, with the SD in each case. Size bars: **A**, 500 µm; **B,** 20 µm**.** * $p<0.05$; ** $p<0.01$

Figure 7 – IGF1 is essential for PC survival in organotypic cultures of the perinatal cerebellum. **A**,**B**, E19.5 wt cerebella were divided in two parts and each hemicerebellum was treated with an IGF1 competitor (H1356 Bachem) (**A**) or vehicle (1x PBS) (**B**), and maintained in culture for 2 days. The number of apoptotic cells is revealed by immunostaining for CaBP and active caspase 3 (AC3). Cell death is sharply increased in competitor-treated slices (plotted in **C,**). **D-G,** cerebella from *Ebf2* null mutants and wt controls were divided in two parts and each hemicerebellum was treated with vehicle (1X PBS in **D,F**) or murine purified IGF1 (**E,G**), and maintained in culture for 2 days. The number of apoptotic PCs was dramatically reduced in IGF1-treated *Ebf2* null slices (**E**) in comparison to vehicle-treated null slices (**D**). Conversely, IGF1 treatment had no effect on cell death in control slices when compared to vehicle treatment (**F** and **G**, respectively). **C,H**, statistical significance of both experiments was estimated computing the ratio of AC3-positive cells located in the PC layer to the total number of CaBP-positive PCs, relative to IGF1 treatment. All treatments were repeated three times for each genotype. The SDs are indicated in all cases examined. *$p<0.05$, **$p<0.01$. Size bar: 50 µm.

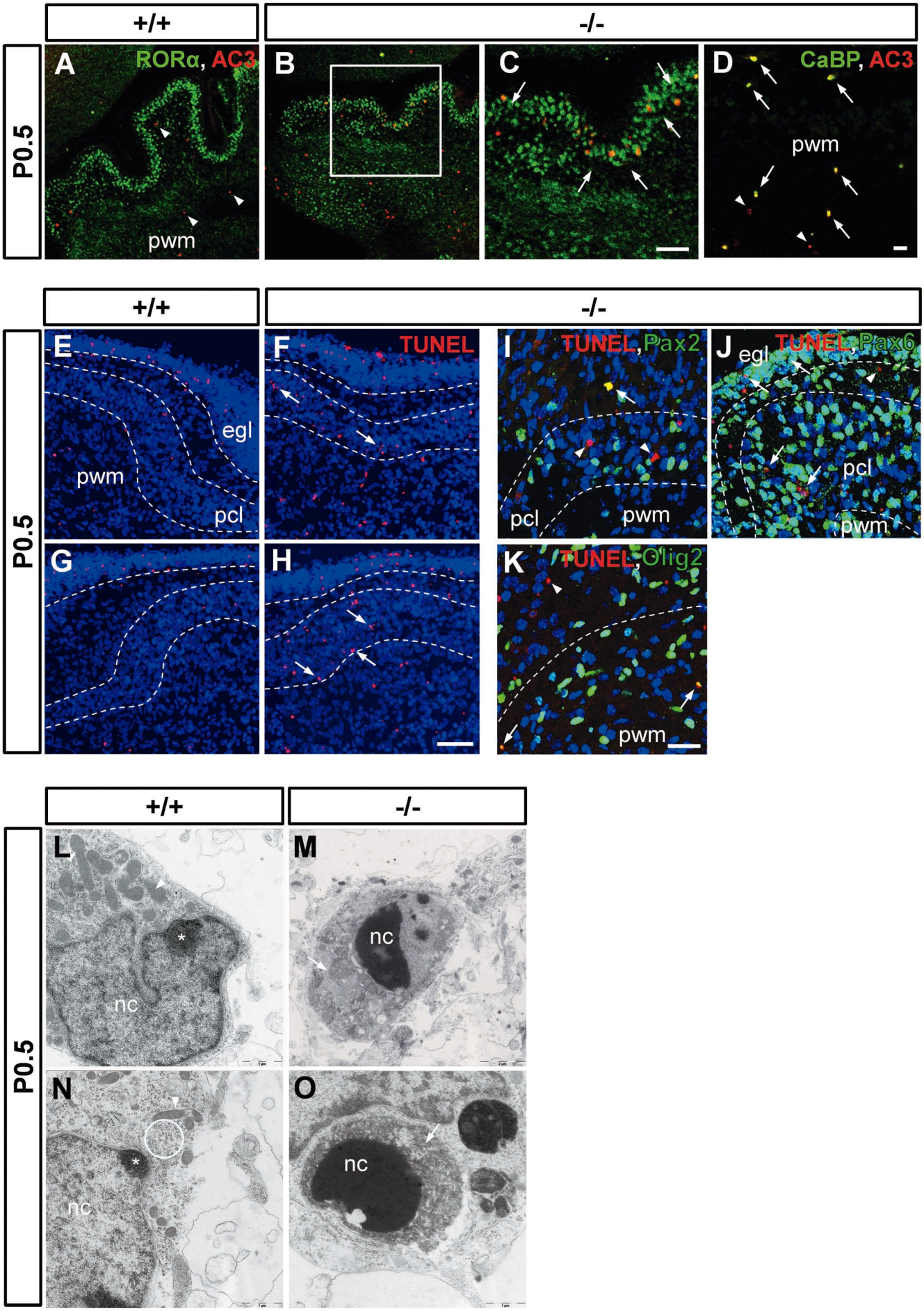
+/+
-/-
P0.5
A
RORα, AC3
pwm
B
C
D
CaBP, AC3
pwm
+/+
-/-
P0.5
E
egl
pwm
pcl
F
TUNEL
I
TUNEL, Pax2
pcl
pwm
J
egl
TUNEL, Pax6
pcl
pwm
G
H
K
TUNEL, Olig2
pwm
+/+
-/-
P0.5
L
*
nc
M
nc
N
*
nc
O
nc

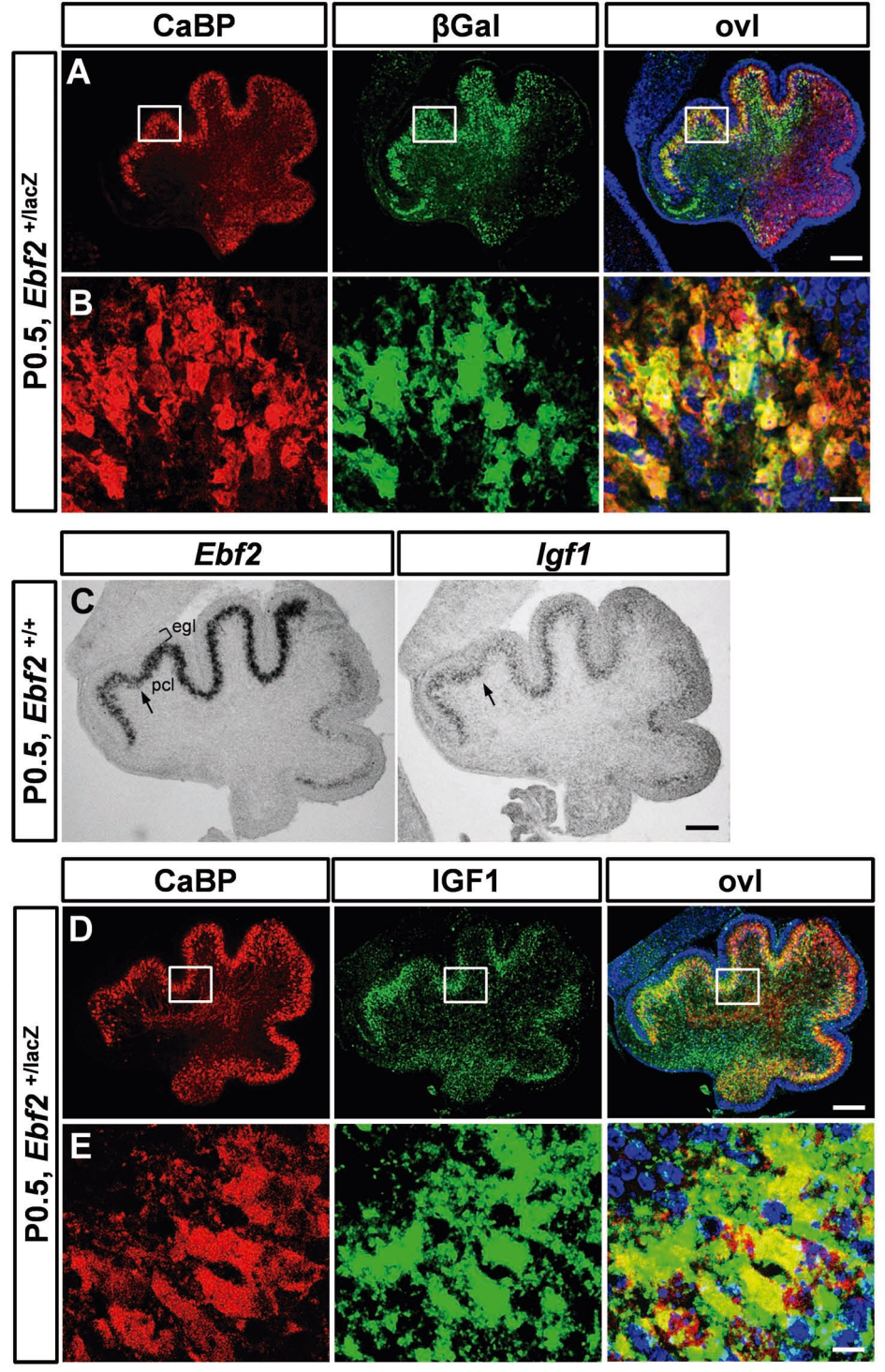
CaBP
βGal
ovl
A
B
P0.5, Ebf2 +/lacZ
Ebf2
Igf1
C
egl
pcl
P0.5, Ebf2 +/+
CaBP
IGF1
ovl
D
E
P0.5, Ebf2 +/lacZ

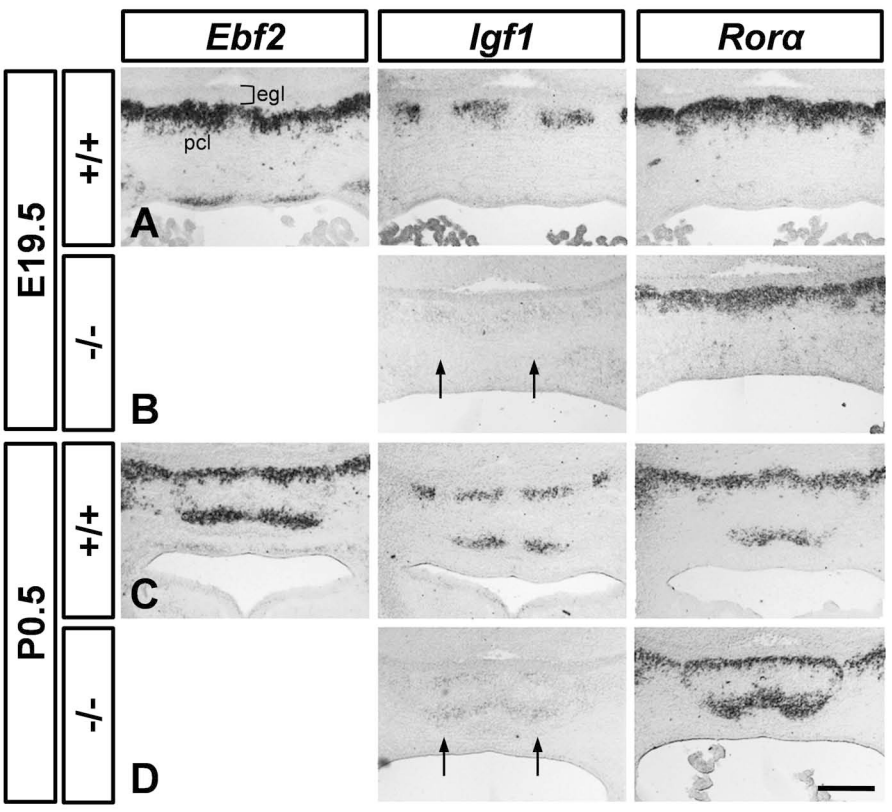
Ebf2
Igf1
Rorα
E19.5
P0.5
+/+
-/-
egl
pcl
A
B
C
D

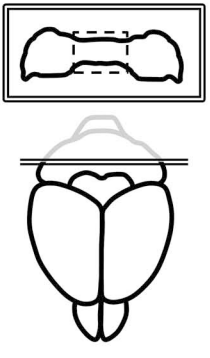

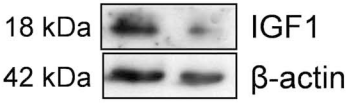
E
18 kDa
42 kDa
IGF1
β-actin

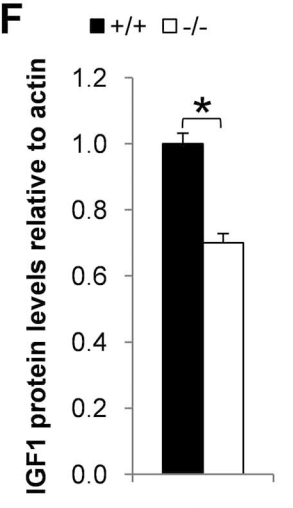
F
+/+
-/-
IGF1 protein levels relative to actin
1.2
1.0
0.8
0.6
0.4
0.2
0.0
*

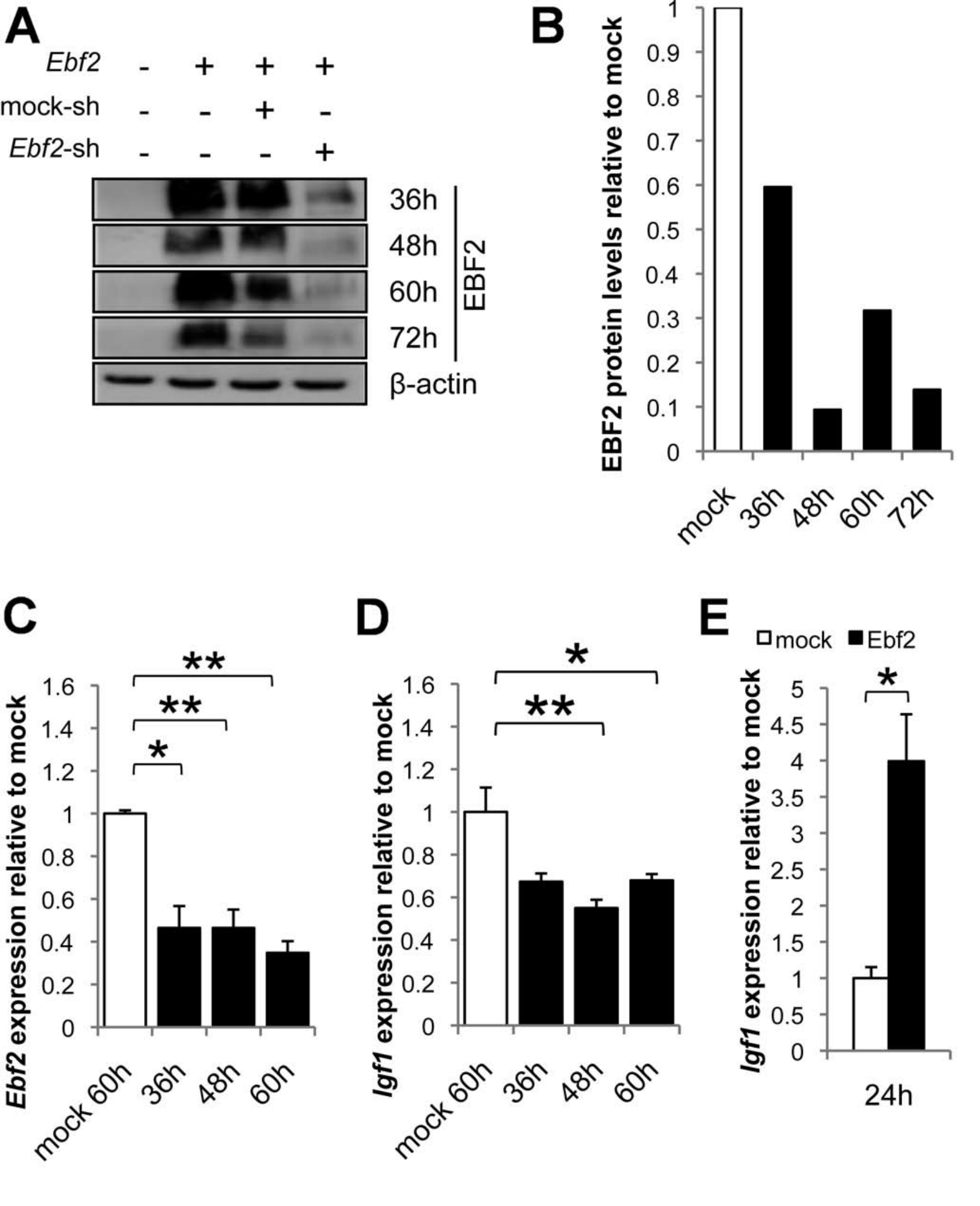
A
Ebf2 - + + +
mock-sh - - + -
Ebf2-sh - - - +
36h
48h
60h
72h
EBF2
β-actin
B
EBF2 protein levels relative to mock
1
0.9
0.8
0.7
0.6
0.5
0.4
0.3
0.2
0.1
0
mock
36h
48h
60h
72h
C
Ebf2 expression relative to mock
1.6
1.4
1.2
1
0.8
0.6
0.4
0.2
0
**
**
*
mock 60h
36h
48h
60h
D
Igf1 expression relative to mock
1.6
1.4
1.2
1
0.8
0.6
0.4
0.2
0
*
**
mock 60h
36h
48h
60h
E
mock
Ebf2
Igf1 expression relative to mock
5
4.5
4
3.5
3
2.5
2
1.5
1
0.5
0
*
24h

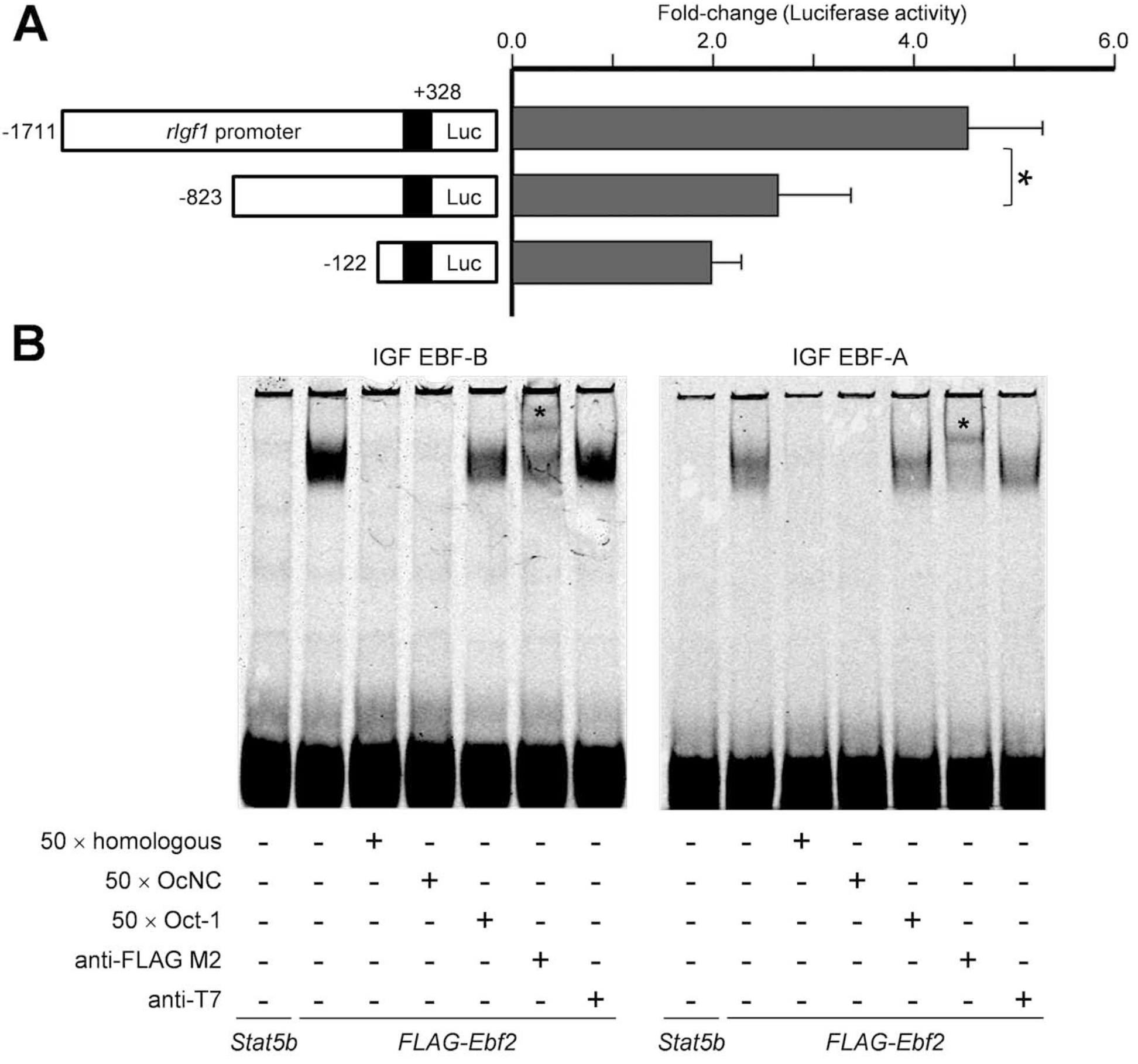
A
Fold-change (Luciferase activity)
0.0
2.0
4.0
6.0
+328
-1711
rlgf1 promoter
Luc
-823
Luc
-122
Luc
*
B
IGF EBF-B
IGF EBF-A
*
*
50 × homologous
50 × OcNC
50 × Oct-1
anti-FLAG M2
anti-T7
Stat5b
FLAG-Ebf2
Stat5b
FLAG-Ebf2

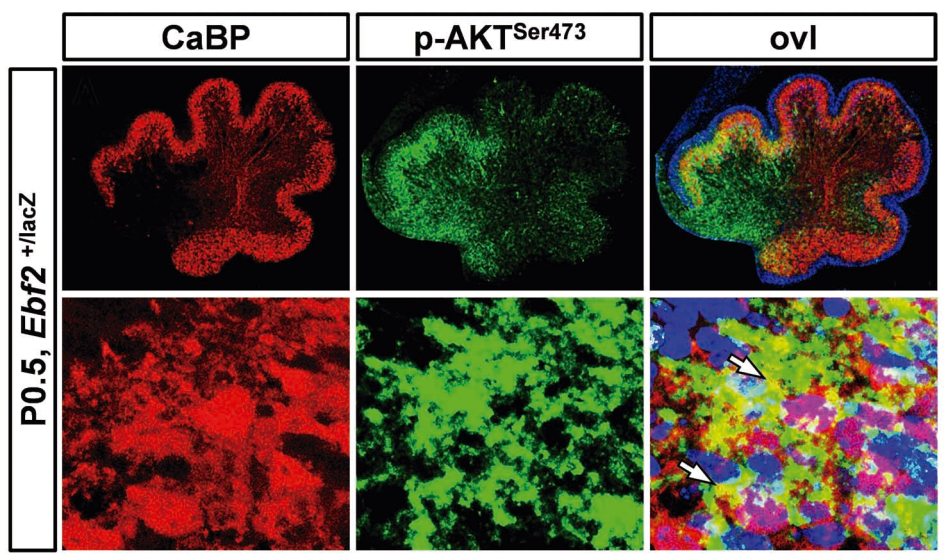
CaBP
p-AKTSer473
ovl
P0.5, Ebf2 +/lacZ

C

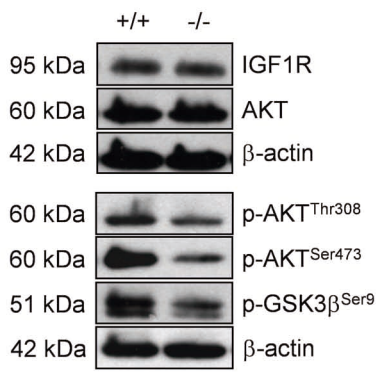
+/+
-/-
95 kDa
IGF1R
60 kDa
AKT
42 kDa
β-actin
60 kDa
p-AKTThr308
60 kDa
p-AKTSer473
51 kDa
p-GSK3βSer9
42 kDa
β-actin

D

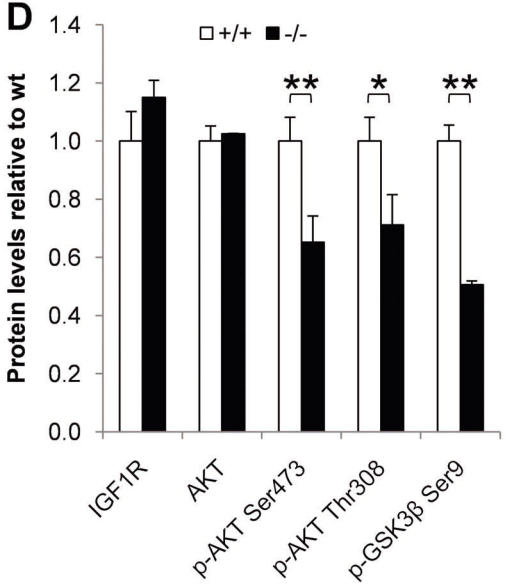
□+/+ ■-/-
Protein levels relative to wt
1.4
1.2
1.0
0.8
0.6
0.4
0.2
0.0
**
*
**
IGF1R
AKT
p-AKT Ser473
p-AKT Thr308
p-GSK3β Ser9

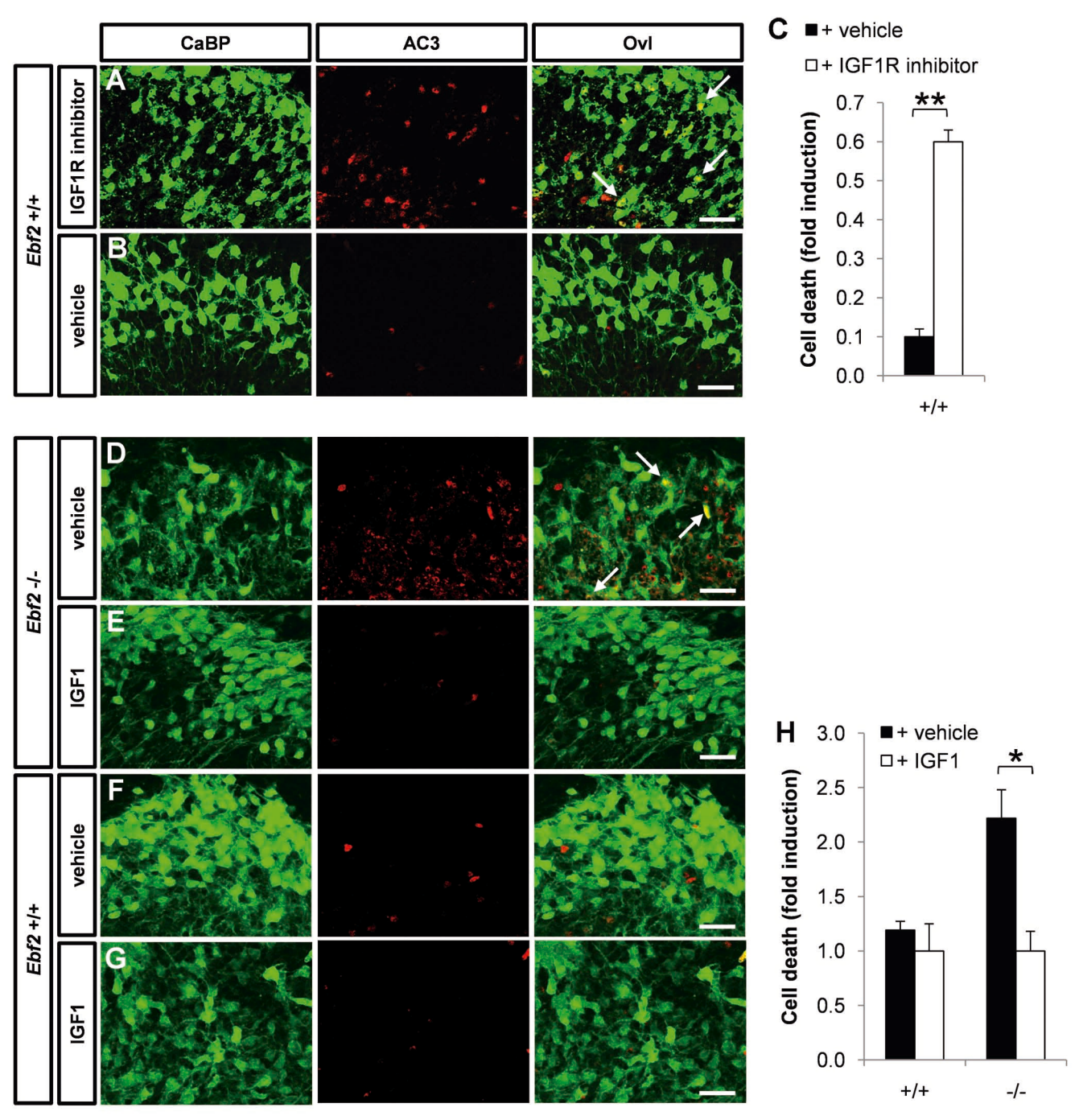
CaBP
AC3
Ovl
Ebf2 +/+
IGF1R inhibitor
vehicle
A
B
C
+ vehicle
+ IGF1R inhibitor
Cell death (fold induction)
0.7
0.6
0.5
0.4
0.3
0.2
0.1
0.0
**
+/+
Ebf2 -/-
vehicle
IGF1
D
E
Ebf2 +/+
vehicle
IGF1
F
G
H
3.0
2.5
2.0
1.5
1.0
0.5
0.0
+ vehicle
+ IGF1
*
Cell death (fold induction)
+/+
-/-